Spectral analysis of the UFBG-based acousto–optical modulator in V–I transmission matrix formalism*

Wu Liang-Ying(吴良英), Pei Li(裴 丽)†, Liu Chao(刘 超), Wang Yi-Qun(王一群), Weng Si-Jun(翁思俊), and Wang Jian-Shuai(王建帅)

Key Laboratory of All Optical Network & Advanced Telecommunication Network of EMC, Beijing Jiaotong Univcnersity, Beijing 100044, *China*

(Received 5 April 2014; revised manuscript received 22 May 2014; published online 24 September 2014)

In this study, the V–I transmission matrix formalism (V–I method) is proposed to analyze the spectrum characteristics of the uniform fiber Bragg grating (FBG)-based acousto–optic modulators (UFBG-AOM). The simulation results demonstrate that both the amplitude of the acoustically induced strain and the frequency of the acoustic wave (AW) have an effect on the spectrum. Additionally, the wavelength spacing between the primary reflectivity peak and the secondary reflectivity peak is proportional to the acoustic frequency with the ratio 0.1425 nm/MHz. Meanwhile, we compare the amount of calculation. For the FBG whose period is M, the calculation of the V–I method is $4\times(2\mathrm{M}-1)$ in addition/subtraction, $8\times(2M-1)$ in multiply/division and $2M$ in exponent arithmetic, which is almost a quarter of the multi-film method and transfer matrix (TM) method. The detailed analysis indicates that, compared with the conventional multi-film method and transfer matrix (TM) method, the V–I method is faster and less complex.

Keywords: uniform fiber bragg grating (UFBG), acousto–optic modulator (AOM), V–I transmission matrix formalism, spectrum

PACS: 07.60.–j, 07.60.Vg, 42.81.Wg **DOI:** 10.1088/1674-1056/23/11/110702

1. Introduction

The fiber Bragg grating (FBG) has been developed into a critical component with wavelength selectivity, which can be used in many devices, such as couplers,[1] lasers,[2] photodetectors,[3] and sensors.[4] In recent years, acousto–optic modulation (AOM) has draw much attention, which can be used in many domains, such as optical add/drop multiplexer (OADM),[5] tunable laser,[6] and filters.[7] In 1997, the uniform fiber Bragg grating-based acousto–optic modulators (UFBG-AOM) was proposed by Liu.[8] In the UFBG-AOM, the longitudinal AW is translated onto the FBG, which changes its transmission characters. The fiber Bragg grating (FBG) in AOM can be excited by an axially propagating extensional AW, which results in high tuning speed, low insertion loss, and simple structure. To be specific, the AW propagating through the UFBG causes the lateral vibration and makes the refractive index of the UFBG periodic stretched and compressed.[9]

Many methods have been proposed to analyze the spectrum of the FBG based device, such as the equilibrium method,[10] the limit method,[11] the method based on coupled-mode theory,[12] the multi-film method,[12] Fourier mode coupling theory,[13–16] and the transfer matrix (TM) method.[17] Among these methods, the Fourier mode coupling theory and the TM method have been applied in analyzing the UFBG-AOM. The Fourier mode coupling theory is easy and fast to analyze the UFBG-AOM, but the effect on the device characteristics from the Bragg construction is not apparent by this method. Even though we can know how the Bragg construction affects the device characteristics through the TM method, the operating rate is limited. In 2003, Capmany proposed a new method, the V–I transmission matrix formalism, to calculate the spectrum of fiber gratings.[18] Compared with the well-known transfer matrix approach, the V–I method is much easier to model photonic devices and circuits without requiring impedance matching, and much faster to calculate the characteristics of the FBG-based device for all the decrease of the number of matrix. Therefore, the V–I method can also be used to analyze the device based on the FBG efficiently.[19]

In this study, the V–I method is applied to analyze the spectrum characteristics of the UFBG-AOM. Compared to the multi-film method and TM method, the proposed V–I method is faster and more succinct. Some relevant simulations are done. From the simulation results, we obtain some important points. The spectral location and intensity of the secondary reflection peaks are set by the acoustic frequency and the amplitude of the acoustically induced strains. The primary reflection peak changes periodically with the acoustically induced strains. In every period, the reflectivity increases at the beginning, and then decreases. The wavelength spacing between the primary reflection peak and the secondary reflection peak is proportional to the acoustic frequency. The number of the secondary reflection peaks increases with the increase of the frequency of induced AW. All these simulation results are con-

*Project supported by the National Natural Science Foundation of China (Grant No. 61275076).

†Corresponding author. E-mail: lipei@bjtu.edu.cn

© 2014 Chinese Physical Society and IOP Publishing Ltd

sistent with the experiment results.[20] The study compares the V–I method with the multi-film method and TM method in the amount of calculation, and points out that the V–I method is faster and more succinct. The results of the V–I method have negligible difference with the results of the multi-film method and TM method.

2. Model and method

2.1. The V–I transmission matrix formalism

For the multi-film method,[12] the FBG are served as a structure with the cascade of multiple-layer optical thin film. A simple example can be seen in Fig. 1, where the left part is an elementary component of the FBG. Here, $E_{m,i}$ and $E_{m,r}(E_{m+1,i}$, and $E_{m+1,r})$ represent the forward and backward propagating fields of the film m $(m+1)$. The study uses $V_m = E_{m,i} + E_{m,r}$ and $I_m = (E_{m,i} - E_{m,r})/Z_m$ to translate the forward and backward propagating fields of the multi-film method into the fields of the V–I method, where Z_m and n_m denote the impedance and the refractive index of the medium m and $Z_m = Z_0/n_m = 120\pi/n_m$. Consequently, the V–I transmission matrix is defined as follows:

$$\begin{bmatrix} V_m \\ I_m \end{bmatrix} = \|VI_m\| \cdot \begin{bmatrix} V_{m+1} \\ I_{m+1} \end{bmatrix}. \tag{1}$$

The VI_m is defined as $VI_m = VI_m^I \cdot VI_m^L$, and the interface matrix VI_m^I is formulated as

$$VI_m^I = \begin{bmatrix} 1 & 0 \\ 0 & 1 \end{bmatrix},$$

which is one of the most important features of the V–I method.

The layer matrix of the transmission matrix VI_m^L for the medium m with the refractive index n_m and length L_m can be defined as

$$VI_m^L = \begin{bmatrix} \cos\sigma_m & \mathrm{j}Z_m \sin\sigma_m \\ \mathrm{j}\dfrac{\sin\sigma_m}{Z_m} & \cos\sigma_m \end{bmatrix}, \quad \sigma_m = \frac{(2\pi)n_m}{\lambda} L_m. \tag{2}$$

Then, to analyze the FBG by the V–I method,[18] the equation can be written as

$$\begin{aligned} \begin{bmatrix} V_1 \\ I_1 \end{bmatrix} &= VI_1^I VI_1^L VI_2^I VI_2^L \cdots VI_m^I VI_m^L \begin{bmatrix} V_{m+1} \\ I_{m+1} \end{bmatrix} \\ &= VI_1^L VI_2^L \cdots VI_m^L \begin{bmatrix} V_{m+1} \\ I_{m+1} \end{bmatrix} \\ &= \prod_{j=i}^{m} \|VI_j^L\| \cdot \begin{bmatrix} V_{m+1} \\ I_{m+1} \end{bmatrix} \\ &= \begin{bmatrix} A & B \\ C & D \end{bmatrix} \cdot \begin{bmatrix} V_{m+1} \\ I_{m+1} \end{bmatrix}. \end{aligned} \tag{3}$$

As a consequence, the reflection and transmission transfer functions can be written as

$$\begin{aligned} t &= \frac{2}{A + B/Z_2 + CZ_1 + DZ_1/Z_2}, \\ r &= \frac{A + B/Z_2 - CZ_1 - DZ_1/Z_2}{A + B/Z_2 + CZ_1 + DZ_1/Z_2}. \end{aligned} \tag{4}$$

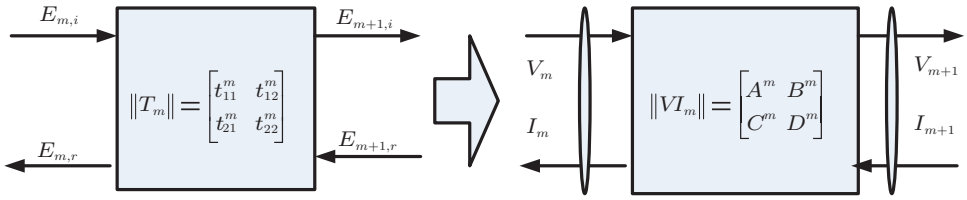


Fig. 1. A simple example of fields changing from the multi-film method to the V–I method.

2.2. UFBG-based AOM

The structure of the UFBG-based AOM is shown in Fig. 2, which is composed of the UFBG, the silica horn, and the piezoelectric transducer (PZT). The voltage source drives the vibration of the PZT, and the silica horn induces the longitudinal AW into the single mode fiber, which makes the uniform FBG periodically stretched and compressed. After propagating over the uniform FBG, the AW will be absorbed by the fiber coating layer.

The strain field of the longitudinal vibration can be written as[21]

$$s(z) = s_0 \sin(k_a z), \quad k_a = 2\pi/\lambda_a, \tag{5}$$

where k_a is the propagation constant of AW, $\lambda_a = v_a/f_a$ is the acoustic wavelength, v_a is the acoustic phase velocity, and f_a is the acoustic frequency. The variable $s_0 = \sqrt{2P_a/(EAv_{ga})}$ is the amplitude of acoustically induced strain, P_a is the power of the acoustic wave in the fiber with Young's modulus E and area A, and v_{ga} is the group velocity of the AW.

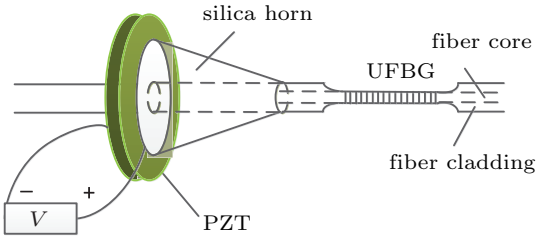


Fig. 2. (color online) The structure of the UFBG-AOM.

After the AW is induced into the uniform FBG, the re-

fractive index perturbation $\Delta n(z)$ changes into[16]

$$\Delta n(z) = \delta_n \left[1 + \cos\left(\frac{2\pi}{\Lambda} z + \frac{\lambda_a}{\Lambda} s_0 \cos(k_a z)\right)\right], \quad 0 \le z \le L, \tag{6}$$

where δ_n is the refractive index modulation depth, L is the length of the grating, and Λ is the period of the grating.

3. Numerical simulations

In this section, the numerical simulation results of UFBG-based AOM in different acoustic frequency and amplitude of acoustically induced strain are given. The parameters of the simulation are shown in Table 1.

Table 1. Simulation parameters.

Variable	Parameter	Simulation value
L	grating length	15 mm
Λ	grating period	525.878 nm
λ_0	central wavelength	1545.1 nm
n_{eff}	effective refractive index	1.4774
δ_n	refractive index modulation depth	0.9×10^{-4}

According to Eqs. (4) and (6), the spectrum of the AOM in different frequencies are given in Fig. 3, where the amplitude of acoustically induced strain is set at $s_0 = 100\mu\varepsilon$ and the acoustic frequency changes from 0.75 MHz to 3.0 MHz.

From Fig. 3, one can conclude that, when there is no AW induced into the grating, the spectrum has only one reflectivity peak at the central length. Once the AW is on, the reflectivity peaks appear at not only the location of the central length, but also the locations of the other lengths. To be specific, only the main reflectivity peak appears in the spectrum in the condition that there is no AW propagating through the UFBG because of the coupling between the forward-propagating core mode and the backward-propagating core mode. However, when the AW is propagated through the FBG, the side bands appear because of the coupling between the AW and a part of the optical wave, and the strength of coupling is changed periodically with the increase of the strain.

Taking Fig. 3(a) for example, except the main reflectivity peak at the central length with the reflectivity of 0.8488, there are still four secondary reflectivity peaks, which are 1544.9 nm with the reflectivity of 0.3385, 1545.09 nm with the reflectivity of 0.8208, 1545.21 nm with 0.8099 and 1545.3 nm with 0.4089. The study defines the two peaks near the primary reflectivity peak as the first-order secondary reflectivity peaks, which are symmetric with respect to the central length.

Comparing Figs. 3(a) and 3(b), we find that with the increase in the frequency of the AW, the reflectivity of the primary reflectivity peak increases from 0.8488 and 0.9676 to 0.9773 and 0.9801. Meanwhile, the reflectivity of the first-order secondary reflectivity peak decreases from the 0.8208 to 0.1876. The increase and decrease of these peaks conform to the law of conservation of power. In addition, figure 3 illustrates that the wavelength spacing between the primary reflectivity peak and the secondary reflectivity peak increases with the frequency of AW.

Then, the study figures out a series of simulation data points, and the linear fitting results are shown in Fig. 4. It is clear that the wavelength spacing $\Delta\lambda$ is proportional to the acoustic frequency, and the ratio is 0.1425 nm/MHz. This calculating ratio is consistent with the experimental result of 0.142 nm/MHz.[20] This means the V–I method, used to analyze the UFBG-AOM, is correct and effective.

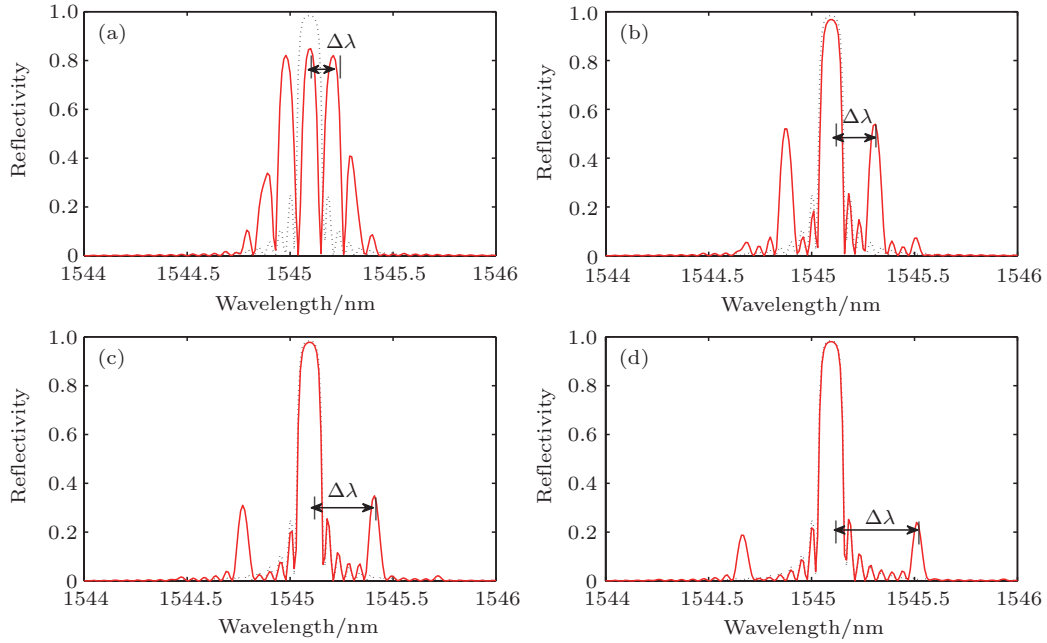


Fig. 3. (color online) Spectrum of UFBG-AOM with different acoustic frequency, where $s_0 = 100\mu\varepsilon$ and $f_a = 0$ (the dotted line), 0.75 MHz (a), 1.5 MHz (b), 2.25 MHz (c), and 3.0 MHz (d).

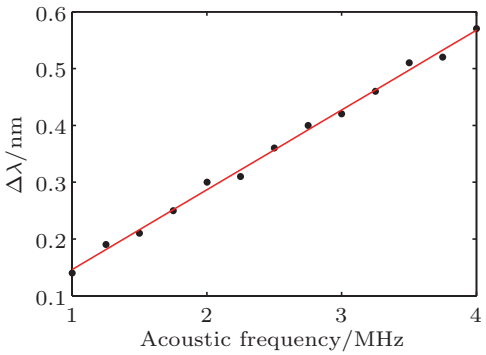


Fig. 4. (color online) Wavelength spacing $\Delta\lambda$ varies with the acoustic frequency. The dots are the calculated data; the solid line fits for the data.

At last, we set the acoustic frequency at 800 kHz, and then obtain the results of setting amplitude of acoustically induced strain at $s_0 = 50\mu\varepsilon$, $100\mu\varepsilon$, $150\mu\varepsilon$, $200\mu\varepsilon$, $250\mu\varepsilon$, and $300\mu\varepsilon$, which can be seen in Fig. 5. It is obvious that under the same acoustic frequency, with an increase of the strain, the number of the secondary reflectivity peak increases.

Comparing the primary reflectivity peaks in Figs. 5(a)–5(f) with each other, it is apparent that the reflectivity of the primary peak changes periodically with the increase of the strain. When the strain increases from $50\mu\varepsilon$ to $200\mu\varepsilon$, the reflectivity decreases from 0.9716 to 0.2049 gradually, while the strain increases from $200\mu\varepsilon$ to $300\mu\varepsilon$, and the reflectivity increases to 0.6491.

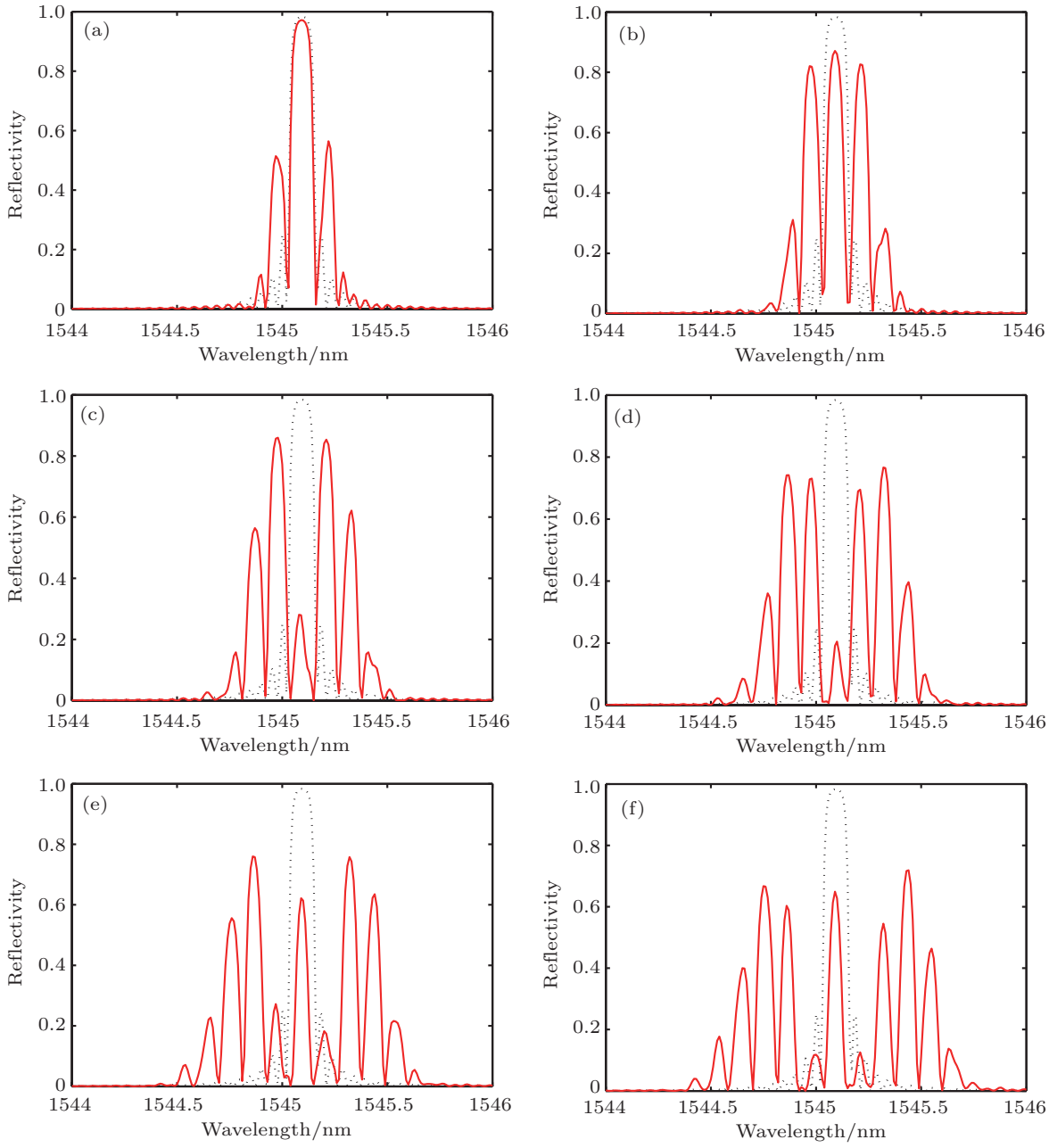


Fig. 5. (color online) Spectrum of UFBG-AOM with different strain, where $f_a = 800$ kHz and $s_0 = 0$ (the dotted line), $50\mu\varepsilon$ (a), $100\mu\varepsilon$ (b), $150\mu\varepsilon$ (c), $200\mu\varepsilon$ (d), $250\mu\varepsilon$ (e), and $300\mu\varepsilon$ (f).

4. Performance evaluation

In order to compare the V–I method with the multi-film method and the TM method, all the parameters are the same. As shown in Fig. 6, when the frequency of the acoustic wave is 2250 kHz and the acoustic amplitude is $100\mu\varepsilon$, the results from the three methods are almost the same, in spite of a little difference shown in the upper right corner. The order of magnitude of the error between the V–I method and the multi-film method is 10^{-4}, and that between the V–I method and the TM method is 10^{-5} (see Fig. 7).

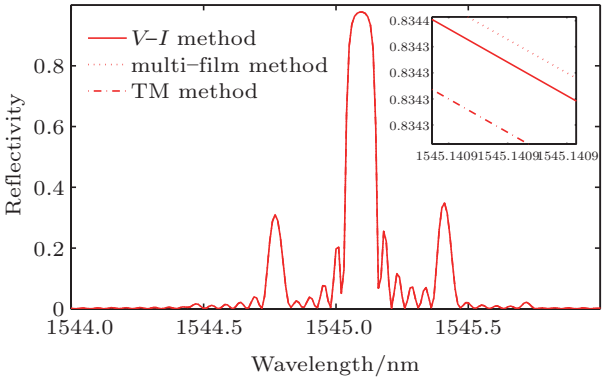


Fig. 6. (color online) Spectrum of the UFBG-AOM in the V–I method (the solid line), the multi-film method (the dotted line), and the TM method (the chain line) when $f_a = 2250$ kHz and $s_0 = 100\mu\varepsilon$.

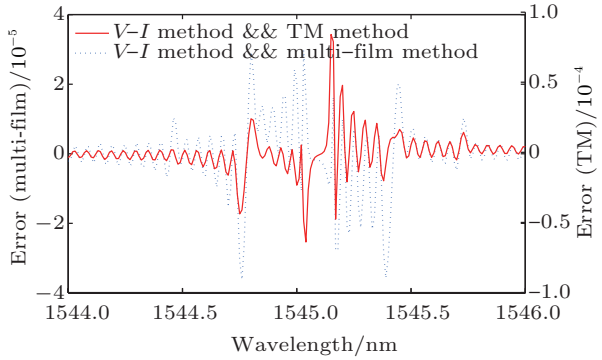


Fig. 7. (color online) The error between the V–I method and the multi-film and TM methods when $f_a = 2250$ kHz and $s_0 = 100\mu\varepsilon$.

Assuming that the number of the period is M, we list the amount of calculation of the three methods respectively in Table 2.

Table 2. Amount of calculation of the three methods.

	add. (+) / sub. (−)	mul. (×) / div. (÷)	exp. (e^{δ})
V–I transmission method	$4\times(2M-1)$	$8\times(2M-1)$	$2M$
Multilayer film method	$12\times(2M-1)$	$13\times(2M-1)$	$8M$
Transfer matrix	$8\times(2M-1)$	$52\times(2M-1)$	$8M$

In terms of the calculation of addition and subtraction, the $4\times(2M-1)$ of the V–I method is lower than the $12\times(2M-1)$ of the multi-film method and the $8\times(2M-1)$ of the TM method. For the multiply and division calculation, the TM method is much more difficult than the V–I and multi-film method, because the $52\times(2M-1)$ is much larger than the $8\times(2M-1)$ and $13\times(2M-1)$. The exponent arithmetic of the V–I method is also easier than the other methods. To be specific, the amount of calculation of the V–I method is about a quarter of the others.

In accordance with the discussion above, we conclude that the results of three methods are almost the same, and the amount of calculation of the V–I method is much lower than the multi-film method and the TM method.

5. Conclusion

The V–I transmission formalism is used to analyze the UFBG-based AOM in this study. By simulation, the study figures out the spectrum fast and effectively. Those simulation results illustrate that the location, the reflectivity and the number of peaks are determined by the acoustic frequency and amplitude. The wavelength spacing between the secondary and the primary reflectivity peaks has a linear relation with the frequency of the acoustic wave. Under the same acoustic frequency, the reflectivity of the primary peak changes periodic with the increase of the amplitude of the acoustically induced strain. All these simulation results are consistent with the experiment results in our former work. This means that the V–I method used to analyze the UFBG-AOM is corrected and effective.

Comparing the simulation results and the amount of calculation of the V–I method, the multi-film method and the TM method, we conclude that the simulation results of the V–I method are almost the same as those of the multi-film method and TM method, because the order of magnitude of the error between the V–I method and the other methods is 10^{-4} and 10^{-5}. However, the amount of calculation of the multi-film method and the TM method is almost four times the calculation amount of the V–I method. Thus, this study concludes that the V–I method is faster and more succinct than the multi-film method and the TM method.

References

[1] Dong X W and Liu W K 2013 *Chin. Phys. B* **22** 024210
[2] Feng T, Yan F P, Li Q, Peng W J, Feng S C, Tan S Y and Wen X D 2013 *Chin. Phys. B* **22** 014208
[3] Guo J C, Zuo Y H, Zhang Y, Ding W C, Cheng B W, Yu J Z and Wang Q M 2009 *Chin. Phys. B* **22** 18 2223
[4] Sun L Q, Dong B, Wang Y X, Evan L and Wang A B 2008 *Chin. Phys. Lett.* **25** 3593
[5] Diez A, Delgado-Pinar M, Mora J, Cruz J L and Andres M V 2003 *IEEE Photon. Technol. Lett.* **15** 84
[6] Russo N A, Duchowicz R, Mora J, Cruz J L and Andres M V 2002 *Opt. Commun.* **210** 361
[7] Fu M Y, Liu W F, Chen T C and Sheng H J 2003 *IEEE Photon. Technol. Lett.* **15** 1392
[8] Liu W F, Russell P S J and Dong L 1997 *Opt. Lett.* **22** 1515

[9] Silva R E, Franco M A, Neves P T, Bartelt H and Pohl A A 2013 *Opt. Express* **21** 6997
[10] Guan B O, Yu Y L, Ge C F and Dong X Y 2000 *Acta Opt. Sin.* **20** 34 (in Chinese)
[11] Born M and Wolf E 1975 *Principles of Optics* (Beijing: Publishing House Of Electronics Industry) p. 422 (in Chinese)
[12] Zhang Z J 2009 *Optic Fiber Grating Theoretical Basis and Sensing Technology* (Beijing: Science Press) p. 100 (in Chinese)
[13] Zeng X K and Rao Y J 2010 *Acta Phys. Sin.* **59** 8597 (in Chinese)
[14] Li Z X, Pei L, Liu C, Ning T G and Yu S W 2012 *Appl. Opt.* **51** 7314
[15] Liu C, Pei L, Li Z X, Ning T G, Yu S W and Kang Z X 2013 *Appl. Opt.* **52** 3318
[16] Liu C, Pei L, Li Z X, Ning T G, Gao S, Kang Z X and Sun J 2013 *Acta Phys. Sin.* **62** 034208 (in Chinese)
[17] Oliveira R A, Neves P T, Pereira J T and Pohl A A A 2008 *Opt. Commun.* **281** 4899
[18] Capmany J, Muriel M A and Sales S 2003 *J. Lightwave Technol.* **21** 3125
[19] Li Z X, Li P, Qi C H, Peng W J, Ning T G, Zhao R F and Gao S 2010 *Acta Phys. Sin.* **59** 8616 (in Chinese)
[20] Delgado-Pinar D Z M, Diez A, Perez-Millan P and Andres M V 2006 *Opt. Express* **14** 1106
[21] Russell P S L and Liu W F 2000 *J. Opt. Soc. Am. A* **17** 1421